Moment-Based Parameter Estimation and Blind Spectrum Sensing for Quadrature Amplitude Modulation

Tao Cui, Jia Tang, Feifei Gao, and Chintha Tellambura, *Senior Member, IEEE*

***Abstract*—Knowing accurate noise variance and signal power is crucial to most spectrum-sensing algorithms such as energy detection, matched filter detection, and cyclostationary detection. In this paper, we consider a practical scenario when these two parameters are unknown and are needed to be estimated before the spectrum sensing. This task is non-trivial without knowing the status of the primary user, and we categorize the related spectrum sensing as a *blind* one. We develop the estimation algorithms for unknown parameters by exploiting the signal constellation of the primary user. Three different parameter estimators that do not require any training are then proposed based on the moments of the received signals. Since the secondary user may not know the primary user's signal constellation, we develop a robust approach that approximates a finite quadrature amplitude modulation (QAM) constellation by a continuous uniform distribution. We also derive the modified Cramér-Rao bound (CRB) for noise variance estimation. Then the optimal moment pair is found from minimizing the mean squared error (MSE) of the signal-to-noise ratio (SNR). The method of choosing the spectrum sensing threshold by taking into consideration the estimation error is also discussed.**

***Index Terms*—Blind spectrum sensing, cognitive radio, noise variance estimation, SNR estimation.**

I. Introduction

With the rapid development of wireless applications, spectrum resources are facing ever increasing demand. In traditional spectrum management, spectrum bands are exclusively allocated to specific licensed users, and unlicensed users are not allowed to access these bands, even when they are not being used at a certain period. This drawback greatly reduces the efficiency of spectrum usage and results in spectrum scarcity. Cognitive radio (CR) [1] is a promising technology to remedy the spectrum scarcity by allowing the unlicensed (secondary) users to opportunistically access the spectrum assigned to the licensed (primary) users, provided that no harmful interference is experienced by the incumbent users.

Because the unlicensed user must reliably detect the existence of the incumbent primary users, the key technique for successfully applying CR is the spectrum sensing. The existing spectrum-sensing techniques include energy detection [2]–[6], cyclostationary detection [7], and wavelet detection [8], of which energy detection is the most promising candidate for practical employment due to its very low computational complexity. Specifically, energy detection compares the average received power with a pre-defined threshold to determine the presence of the primary user. The detection threshold is related to the false alarm probability, and is a function of both the noise variance and the signal power. In most works, these two parameters are assumed perfectly known [3]. Although, in the absence of the primary user, the noise variance can be estimated from the average received power, the *a priori* knowledge of the existence of the primary user is never possible before executing the spectrum sensing, and this situation becomes a *chicken and egg* problem.

In this paper, we consider the blind spectrum sensing problem by treating both the signal power of the primary user and the noise variance as unknown parameters that are to be estimated before knowing the status of the primary user. Motivated by the signal-to-noise ratio (SNR) estimators in [9]–[11], we propose to estimate the unknown parameters by using three different approaches; the direct estimator, approximate maximum likelihood (ML) estimator, and pseudo-linear minimum mean square error (MMSE) estimator. We find that the signal structure of the primary user is crucial to the estimators' performance. Furthermore, since the constellation used by the primary user may not be known to the secondary user, we utilize a robust approach that approximates binary phase-shift keying (BPSK) or a finite quadrature amplitude modulation (QAM) constellation by a continuous uniform distribution. The modified Cramér-Rao bound (CRB) for noise variance estimation is also derived and the optimal moment pair is found by minimizing the mean square error (MSE) of the SNR. Moreover, we propose a modified energy detector by using the estimated SNR, discuss the effects of the estimation errors on spectrum sensing, and provide several approaches to choose the detection threshold under estimation errors.

The rest of this paper is organized as follows. In Section II, we briefly review the model of the cognitive network as well as the energy detector. In Section III, we propose three signal

Paper approved by H. Arslan, the Editor for Cognitive Radio and OFDM of the IEEE Communications Society. Manuscript received November 3, 2009; revised June 19, 2010.

This paper has been presented in part at the IEEE Wireless Communications and Networking Conference, Sydney, Australia, April 2010.

T. Cui is with the Department of Electrical Engineering, California Institute of Technology, Pasadena, CA 91125, USA (e-mail: taocui@caltech.edu).

F. Gao is with the School of Engineering and Science, Jacobs University, Bremen, Germany (e-mail: feifeigao@ieee.org).

J. Tang is with Qualcomm Inc. 3165 Kifer Road, Santa Clara, CA 95051, USA (e-mail: jiat@qualcomm.com).

C. Tellambura is with the Department of Electrical and Computer Engineering, Edmonton, Alberta, T6G 2V4, Canada (e-mail: chintha@ece.ualberta.ca).

Digital Object Identifier 10.1109/TCOMM.2010.120710.090667

power and noise variance estimators. In addition, spectrum sensing in the presence of the estimation errors is discussed in this section. In Section IV, we derive the modified CRB and optimize the moment pair. The simulation results are given in Section V and conclusions are made in Section VI.

II. System Model

We consider a simple cognitive network with one secondary user and one primary user, denoted by $\mathbb{U}$ and $\mathbb{P}$, respectively. The received signal by $\mathbb{U}$ at time i is

$$y_i = \theta e^{\jmath(\epsilon i+\phi)} x_i h_i + \sigma w_i, \tag{1}$$

where $\theta \in \{0,1\}$ is the primary user indicator, x_i is the transmitted signal from $\mathbb{P}$, h_i is the Rayleigh channel gain between $\mathbb{P}$ and $\mathbb{U}$ (a real number), w_i is white Gaussian noise with zero mean and unit variance, σ is the noise variance, and ϵ and ϕ are the frequency offset and the phase offset, respectively.[1] To keep the discussion general, we assume that ϵ and ϕ are unknown to the secondary user. Moreover, the signal constellation $\mathcal{C}$ contains M elements $c_1, \ldots, c_M$ and has zero mean and unit energy.

Assume N consecutive symbols are observed at $\mathbb{U}$, during which period both h_i and θ remain unchanged. For simplicity, we denote h_i as h. Taking WCDMA as an example, the constant channel can be assumed in each subframe (2 ms), which contains 960 symbols [12]. The probability density function (pdf) of y_i given ϵ and ϕ is

$$\begin{aligned}
&\Pr(y_1,\ldots,y_N|\theta=0,\epsilon,\phi) = \frac{1}{(2\pi)^N\sigma^{2N}} e^{-\frac{\sum_{i=1}^N |y_i|^2}{\sigma^2}},\\
&\Pr(y_1,\ldots,y_N|\theta=1,\epsilon,\phi) =\\
&\qquad \frac{1}{(2\pi)^N\sigma^{2N}} \prod_{i=1}^N \sum_{x_i\in\mathcal{C}} e^{-\frac{|y_i - e^{\jmath(\epsilon i+\phi)}hx_i|^2}{\sigma^2}} \Pr(x_i).
\end{aligned} \tag{2}$$

The optimal detector is derived from the likelihood ratio test:

$$\begin{aligned}
&\Lambda(y_1,\ldots,y_N|\epsilon,\phi) = \frac{\Pr(y_1,\ldots,y_N|\theta=1,\epsilon,\phi)}{\Pr(y_1,\ldots,y_N|\theta=0,\epsilon,\phi)}\\
&= \prod_{i=1}^N \sum_{x_i\in\mathcal{C}} e^{-\frac{|hx_i|^2 - 2\Re\{y_i^* e^{\jmath(\epsilon i+\phi)}hx_i\}}{\sigma^2}} \Pr(x_i),
\end{aligned} \tag{3}$$

where $\Re\{\cdot\}$ denotes the real part of the operand.

In the following, we focus on the energy detector that compares $\sum_{i=1}^N |y_i|^2$ with a threshold λ. If $\sum_{i=1}^N |y_i|^2 > \lambda$, then the secondary user decides $\hat{\theta} = 1$; otherwise, the decision $\hat{\theta} = 0$ will be made. There are two reasons why we consider energy detector. First, in low SNR, by assuming $\frac{|hx_i|^2 - 2\Re\{y_i^* e^{\jmath(\epsilon i+\phi)}hx_i\}}{\sigma^2} \ll 1$ and using Taylor series expansion $e^x \approx 1 + x + \frac{x^2}{2}$, it can be shown that the energy detector $\sum_{i=1}^N |y_i|^2$ is nearly optimal. Second, if x_i is considered as Gaussian with zero mean and unit variance,[2] then it is easy to verify that $\Lambda(y_1,\ldots,y_N|\epsilon,\phi)$ in (2) is a strictly increasing function in $\sum_{i=1}^N |y_i|^2$. Hence, energy detector is again optimal. Note that $\Lambda(y_1,\ldots,y_N|\epsilon,\phi)$ is not affected by the synchronization errors ϵ and ϕ.

The key metrics in spectrum sensing are the probability of detection and the probability of false alarm, defined as

$$P_d = \Pr(\hat{\theta}=1|\theta=1), \quad P_f = \Pr(\hat{\theta}=1|\theta=0). \tag{4}$$

Since $\sum_{i=1}^N |y_i|^2$ is a central chi-square random variable when $\theta = 0$ and is a non-central chi-square random variable when $\theta = 1$, the probability of false alarm can be obtained as

$$P_f(\lambda) = \int_\lambda^{+\infty} \frac{1}{\sigma^{2N}\Gamma(N)} t^{N-1} \exp\left(-\frac{t}{\sigma^2}\right) dt = \frac{\Gamma\left(N, \frac{\lambda}{\sigma^2}\right)}{\Gamma(N)}, \tag{5}$$

and the probability of detection is

$$\begin{aligned}
P_d(\lambda) = &\sum_{x_1,\ldots,x_N\in\mathcal{C}} \prod_{i=1}^N \Pr(x_i) \frac{1}{\Gamma(N)}\\
&\times \sum_{j=0}^{\infty} e^{-\xi(x_1,\ldots,x_N)} \frac{\xi^j(x_1,\ldots,x_N)}{j!} \Gamma(N+2j,\lambda),
\end{aligned} \tag{6}$$

where $\Gamma(\cdot,\cdot)$ is the upper incomplete gamma function, $\Gamma(\cdot)$ is the gamma function, and

$$\xi(x_1,\ldots,x_N) = \frac{h^2}{\sigma^2} \sum_{i=1}^N |x_i|^2. \tag{7}$$

A typical practical design strategy is to fix the false alarm probability and then try to maximize the detection probability, i.e., the constant false alarm rate detector. Thus, let the false alarm probability $P_f(\lambda) = \zeta$. We can find the threshold λ and compute the corresponding correct detection probability using (6). The value of the threshold ζ depends on σ and h which are assumed known in many existing works, e.g., [3]. In practice, however, all these parameters have to be obtained from the estimation. In cognitive radio scenario, estimating σ is difficult because we do not know the presence of the primary user; namely, θ is unknown.

To overcome this problem, θ and σ are directly estimated from the received signals in our proposed approach. To this end, let us define $\tilde{\lambda} = \lambda/\sigma^2$. Then, the probability of false alarm (5) depends on $\tilde{\lambda}$ only, while the probability of detection (6) depends on $\tilde{\lambda}$ and SNR $\rho = \frac{h^2}{\sigma^2}$ only. Therefore, the presence of the primary user can be determined by comparing the estimated SNR with $\tilde{\lambda}$. The problem is therefore equivalent to estimating σ^2 and SNR (or, equivalently, σ and h) by using only the received signals. Because of this equivalence, energy detection combined with the parameter estimation will be categorized as a type of *blind energy detection*.

III. Noise Variance Estimation and Blind Spectrum Sensing

In this section, we derive several non-data-aided noise variance and signal power estimators and then propose the blind spectrum sensing algorithm.

[1] In the CR scenario, achieving perfect synchronization between the secondary user and the primary user is difficult.

[2] This assumption is applied to show the optimality of energy detector. We do not make this assumption in the remaining paper.

A. ML Noise Variance Estimation

We first consider the ML estimation of h and σ to gain insight into the structure of the estimator. Note that, if we can estimate θh, then θ can be readily obtained with a threshold detector. With a slight abuse of notation, we will still use h to represent θh. This strategy is crucial to avoid the chicken-egg problem by considering θh as a single parameter. The joint pdf of $y_1, \ldots, y_N$ given h, σ, ϵ and ϕ is

$$p\left(y_1, \ldots, y_N | h, \sigma, \epsilon, \phi\right) = \frac{1}{\pi^N \sigma^{2N}} \prod_{i=1}^{N} \sum_{x_i \in \mathcal{C}} \Pr(x_i) \exp\left(-\frac{\left|y_i - e^{\jmath(\epsilon i+\phi)} h x_i\right|^2}{\sigma^2}\right). \quad (8)$$

For BPSK with $\mathcal{C} = \{1, -1\}$ and $\Pr(1) = \Pr(-1) = \frac{1}{2}$, we have

$$p\left(y_1, \ldots, y_N | h, \sigma, \epsilon, \phi\right) = \frac{1}{\pi^N \sigma^{2N}} \prod_{i=1}^{N} \exp\left(-\frac{|y_i|^2 + |h|^2}{\sigma^2}\right) \cosh \frac{2\Re\{e^{\jmath(\epsilon i+\phi)} h y_i^*\}}{\sigma^2}. \quad (9)$$

The ML estimates of h, σ, ϵ and ϕ are obtained by maximizing the joint pdf in (9). As ϵ, ϕ appear in each of the terms in (9), the closed-form solution for ϵ, ϕ is complicated. Instead, we define $\psi_i = \epsilon i + \phi$ and maximize each term in (9) over ψ_i individually. This action yields

$$\psi_i = \angle h y_i^*. \quad (10)$$

Substituting (10) into (9), we obtain

$$p\left(y_1, \ldots, y_N | h, \sigma\right) = \frac{1}{\pi^N \sigma^{2N}} \prod_{i=1}^{N} \exp\left(-\frac{|y_i|^2 + |h|^2}{\sigma^2}\right) \cosh \frac{2|h y_i^*|}{\sigma^2}. \quad (11)$$

Taking the derivative of $\log p\left(y_1, \ldots, y_N | h, \sigma\right)$ with respect to h and setting the resulting equation to zero, we get

$$h = \sum_{i=1}^{N} \frac{1}{N} \tanh \frac{|h y_i^*|}{\sigma^2} |y_i| \approx \frac{\sum_{i=1}^{N} |y_i|}{N}, \quad (12)$$

where the approximation holds for high SNR. Taking the derivative of $\log p\left(y_1, \ldots, y_N | h, \sigma\right)$ with respect to σ and substituting (12) into the resulting equation, we obtain

$$\begin{aligned} \sigma^2 =& \frac{\sum_{i=1}^{N} |y_i|^2 + N h^2 - 2h \sum_{i=1}^{N} |y_i| \tanh \frac{|h y_i^*|}{\sigma^2}}{N} \\ \approx& \frac{\sum_{i=1}^{N} |y_i|^2}{N} - \left(\frac{\sum_{i=1}^{N} |y_i|}{N}\right)^2. \end{aligned} \quad (13)$$

After obtaining h and σ^2, the SNR can be estimated from

$$\rho = \frac{h^2}{\sigma^2} = \frac{\left(\frac{\sum_{i=1}^{N} |y_i|}{N}\right)^2}{\frac{\sum_{i=1}^{N} |y_i|^2}{N} - \left(\frac{\sum_{i=1}^{N} |y_i|}{N}\right)^2}. \quad (14)$$

Hence, the SNR estimate depends on the amplitude $\bar{A}$ and energy $\bar{E}$, defined as

$$\bar{A} = \frac{\sum_{i=1}^{N} |y_i|}{N} \quad \bar{E} = \frac{\sum_{i=1}^{N} |y_i|^2}{N}. \quad (15)$$

The SNR estimator (14) is similar to the squared signal-to-noise variance (SNV) estimator in [9] for real systems. Our results show that the SNV estimator is an approximate ML estimator for BPSK even in complex systems and in the presence of synchronization errors. Different from SNR estimation, we, here, are interested in estimating h, σ rather than ρ.

When x_i is also Gaussian, (8) becomes

$$p\left(y_1, \ldots, y_N | h, \sigma\right) = \frac{1}{\pi^N (h^2 + \sigma^2)^N} \prod_{i=1}^{N} \exp\left(-\frac{|y_i|^2}{h^2 + \sigma^2}\right). \quad (16)$$

By maximizing $p\left(y_1, \ldots, y_N | h, \sigma\right)$, we can obtain $h^2 + \sigma^2$ only, but not h and σ separately. Therefore, the ML estimator cannot be used for Gaussian signals. Thus, the structure of the signal constellation is crucial for estimating h and σ.

B. Suboptimal Noise Variance Estimation

For higher-order constellations, deriving or approximating the ML estimator in closed-form is difficult. The approximate ML estimator for BPSK uses the two moments $E\{|y_i|\}$ and $E\{|y_i|^2\}$. Motivated by this use of the moments, we then propose to use a high-order moment estimator to approximate the ML estimator.

First, we note that

$$\begin{aligned} |y_i|^k &= \left|\theta e^{\jmath(\epsilon i+\phi)} x_i h_i + \sigma w_i\right|^k \\ &= \left|\theta x_i h_i + \sigma \underbrace{e^{-\jmath(\epsilon i+\phi)} w_i}_{\tilde{w}_i}\right|^k, \; k = 1, 2, \end{aligned} \quad (17)$$

where $\tilde{w}_i = e^{-\jmath(\epsilon i+\phi)} w_i$ has the same distribution as w_i. Therefore, the synchronization error does not change the statistic of $|y_i|^k$ and will be omitted in the rest of the paper.

The pdf of $|y_i|$ is a mixed Ricean distribution and is given by

$$f_{|y_i|}(|y_i|) = \sum_{x_i \in \mathcal{C}} \Pr(x_i) \frac{2|y_i|}{\sigma^2} \times \exp\left(-\frac{|h|^2 |x_i|^2}{\sigma^2} - \frac{|y_i|^2}{\sigma^2}\right) I_0\left(\frac{2|y_i||h x_i|}{\sigma^2}\right), \quad (18)$$

where $I_0(\cdot)$ is the zero-order modified Bessel function of the first kind. The k-th moment of the mixed Ricean distribution in (18) is [11]

$$E\{|y_i|^k\} = h^k \sum_{x_i \in \mathcal{C}} \Pr(x_i) \frac{1}{2^{\frac{k}{2}}} \rho^{-\frac{k}{2}} \Gamma\left(\frac{k}{2} + 1\right) \times \exp\left(-\rho |x_i|^2\right) {}_1F_1\left(\frac{k}{2} + 1; 1; \rho |x_i|^2\right), \quad (19)$$

where ${}_1F_1(\cdot;\cdot;\cdot)$ is the confluent hypergeometric function, and $\Gamma(\cdot)$ is the gamma function.

1) When k is even, we can compute $E\{|y_i|^k\}$ in an alternate

form, i.e.,

$$E\{|y_i|^k\} = \frac{1}{2\pi\sigma^2}\sum_{x_i\in\mathcal{C}}\Pr(x_i)\int |t+hx_i|^k e^{-\frac{|t|^2}{\sigma^2}}dt$$
$$=\frac{1}{2\pi\sigma^2}\sum_{u_i+jv_i\in\mathcal{C}}\Pr(u_i+jv_i)\sum_{j=0}^{\frac{k}{2}}\binom{\frac{k}{2}}{j}$$
$$\times\int\int_{-\infty}^{\infty}(t_1+hu_i)^{2j}(t_2+hv_i)^{k-2j}e^{-\frac{t_1^2+t_2^2}{\sigma^2}}dt_1dt_2. \quad (20)$$

Define

$$G(hz,k,\sigma) = \frac{1}{\sqrt{2\pi\sigma^2}}\int_{-\infty}^{\infty}(t+hz)^k\exp\left(-\frac{t^2}{\sigma^2}\right)dt$$
$$=\sum_{j=0}^{k/2}\binom{k}{2j}(hz)^{k-2j}\frac{(2j)!}{2^{2j}j!}\sigma^{2j}. \quad (21)$$

Equation (20) can be rewritten as

$$E\{|y_i|^k\} = \sum_{u_i+jv_i\in\mathcal{C}}\Pr(u_i+jv_i)$$
$$\times\sum_{j=0}^{\frac{k}{2}}\binom{\frac{k}{2}}{j}G(hu_i,2j,\sigma)G(hv_i,k-2j,\sigma). \quad (22)$$

2) When k is odd, we must compute $E\{|y_i|^k\}$ from (19).

From (20)-(22), we find that the k-th moment can be written as

$$m_k = E\{|y_i|^k\} = h^k f_k(\rho), \quad (23)$$

where $f_k(\rho)$ is a function depending only on modulation and ρ. Therefore, we have

$$\frac{\prod_{p=1}^{P}E\{|y_i|^{k_p}\}}{\prod_{q=1}^{Q}E\{|y_i|^{\kappa_q}\}} = \frac{\prod_{p=1}^{P}f_{k_p}(\rho)}{\prod_{q=1}^{Q}f_{\kappa_q}(\rho)} = F(\rho), \quad (24)$$

if $\sum_{p=1}^{P}k_p = \sum_{q=1}^{Q}\kappa_q$. For any SNR, we can optimize $\{k_p\}$ and $\{\kappa_q\}$ by minimizing the average MSE as discussed in Section IV-B.

1) Direct Estimator: Without considering the distribution of $\sum_{i=1}^{N}|y_i|^k$, the direct SNR estimator can be obtained by replacing $E\{|y_i|^k\}$ with its time average $\frac{1}{N}\sum_{i=1}^{N}|y_i|^k$, i.e.,

$$\hat{\rho} = F^{-1}\left(\frac{\prod_{p=1}^{P}\sum_{i=1}^{N}|y_i|^{k_n}}{\prod_{q=1}^{Q}\sum_{i=1}^{N}|y_i|^{\kappa_q}}\right), \quad (25)$$

where $\sum_{p=1}^{P}k_p = \sum_{q=1}^{Q}\kappa_q$ and $k_p \neq \kappa_q$ for any $1\le p\le P$ and $1\le q\le Q$. After estimating $\hat{\rho}$, we can obtain

$$\hat{h} = \sqrt{\hat{\rho}}\sum_{l=1}^{L}\alpha_l\sqrt[k_l]{\frac{E\{|y_i|^{k_l}\}}{f_{k_l}(\hat{\rho})}}, \quad \hat{\sigma} = \sum_{l=1}^{L}\beta_l\sqrt[k_l]{\frac{E\{|y_i|^{k_l}\}}{f_{k_l}(\hat{\rho})}}, \quad (26)$$

where α_l and β_l are weights to balance the different moments, and $\sum_{l=1}^{L}\alpha_l = \sum_{l=1}^{L}\beta_l = 1$.

2) Moment ML Estimator: As shown in Section III-A, the exact ML estimator is complicated. Instead of using it, we consider two statistics: $\hat{m}_p = \frac{1}{N}\sum_{i=1}^{N}|y_i|^p$ and $\hat{m}_q = \frac{1}{N}\sum_{i=1}^{N}|y_i|^q$. The exact pdf's of $\hat{m}_p$ and $\hat{m}_q$ are hard to derive. Considering the central limit theorem, we can approximate $\hat{m}_p$ and $\hat{m}_q$ as Gaussian random variables. Then the corresponding means are

$$m_p = E\{\hat{m}_p\} = \sigma^p f_p(\rho), \qquad m_q = E\{\hat{m}_q\} = \sigma^q f_q(\rho),$$
$$E\{|\hat{m}_p|^2\} = \frac{1}{N}\sigma^{2p}\left(f_{2p}(\rho)+(N-1)f_p^2(\rho)\right),$$
$$E\{|\hat{m}_q|^2\} = \frac{1}{N}\sigma^{2q}\left(f_{2q}(\rho)+(N-1)f_q^2(\rho)\right),$$
$$E\{\hat{m}_p\hat{m}_q\} = \frac{1}{N}\sigma^{p+q}\left(f_{p+q}(\rho)+(N-1)f_p(\rho)f_q(\rho)\right), \quad (27)$$

while the variances and covariances are

$$\nu_p = E\{|\hat{m}_p|^2\} - E\{|\hat{m}_p|\}^2$$
$$=\frac{1}{N}\sigma^{2p}\left(f_{2p}(\rho)-f_p^2(\rho)\right) = \sigma^{2p}g_{p,p}(\rho,N)$$
$$\nu_q = E\{|\hat{m}_q|^2\} - E\{|\hat{m}_q|\}^2$$
$$=\frac{1}{N}\sigma^{2q}\left(f_{2q}(\rho)-f_q^2(\rho)\right) = \sigma^{2q}g_{q,q}(\rho,N)$$
$$\eta_{p,q} = E\{\hat{m}_p\hat{m}_q\} - E\{\hat{m}_p\}E\{\hat{m}_q\}$$
$$=\frac{\sigma^{p+q}}{N}\left(f_{p+q}(\rho)-f_p(\rho)f_q(\rho)\right) = \sigma^{p+q}g_{p,q}(\rho,N). \quad (28)$$

The joint distribution of $\hat{m}_p, \hat{m}_q$ conditioned on σ and ρ is written as (29) on the top of next page. Then $\hat{m}_p, \hat{m}_q$ can be found by maximizing $\psi(\hat{m}_p,\hat{m}_q|\sigma,\rho)$. For each given ρ, the optimal $\sigma^*(\rho)$ is obtained from the root of the partial derivative of $\psi(\hat{m}_p,\hat{m}_q|\sigma,\rho)$ with respect to σ, i.e., (30) on the top of next page, which is polynomial in σ. If several positive roots exist, we may choose the one that is close to that estimated from (13) or (26). We substitute $\sigma^*(\rho)$ back into (29) and then $\psi(\hat{m}_p,\hat{m}_q|\sigma^*(\rho),\rho)$ is a function of ρ only. Maximizing this function over ρ near that in (12) or (26) yields the approximate ML estimate ρ^*, from which we further obtain the ML estimates $\sigma^*(\rho^*)$ and $h^* = \sigma^*(\rho^*)\sqrt{\rho^*}$. This procedure can be implemented by using a one-dimensional grid search.

3) Approximate Moment ML Estimator: The estimator based on (29) is complicated because the estimations of ρ and σ are coupled. We further consider a decoupled ML estimator by using the following special statistic,

$$\hat{F} = \frac{\hat{m}_p^q}{\hat{m}_q^p} = \frac{(m_p+\epsilon_p)^q}{(m_q+\epsilon_q)^p} \approx \frac{m_p^q}{m_q^p} + \frac{qm_p^{q-1}}{m_q^p}\epsilon_p - \frac{pm_p^q}{m_q^{p+1}}\epsilon_q, \quad (31)$$

where ϵ_p and ϵ_q are errors between $\hat{m}_p$, $\hat{m}_q$ and m_p, m_q and the approximation follows from the first order Taylor's expansion. The variance of $\hat{F}$ can be computed as

$$\nu_F(\rho,N) = E\left\{\left|\frac{qm_p^{q-1}}{m_q^p}\epsilon_p - \frac{pm_p^q}{m_q^{p+1}}\epsilon_q\right|^2\right\}$$
$$=F^2(\rho)\left(\frac{q^2g_{p,p}(\rho,N)}{f_p^2(\rho)} + \frac{p^2g_{q,q}(\rho,N)}{f_q^2(\rho)} - \frac{2pqg_{p,q}(\rho,N)}{f_p(\rho)f_q(\rho)}\right), \quad (32)$$

$$\begin{aligned}\psi(\hat{m}_p,\hat{m}_q|\sigma,\rho) =&\frac{1}{2\pi\sqrt{\nu_p\nu_q-\eta_{p,q}^2}}\exp\left(-\frac{\nu_q(\hat{m}_p-m_p)^2+\nu_p(\hat{m}_q-m_q)^2-2\eta_{p,q}(\hat{m}_p-m_p)(\hat{m}_q-m_q)}{2(\nu_p\nu_q-\eta_{p,q}^2)}\right)\\ =&\frac{\exp\left(-\frac{1}{2(1-\xi^2(\rho,N))}\left(\frac{(\hat{m}_p-m_p)^2}{\sigma^{2p}g_{p,p}(\rho,N)}+\frac{(\hat{m}_q-m_q)^2}{\sigma^{2q}g_{q,q}(\rho,N)}-\frac{2\xi(\rho,N)(\hat{m}_p-m_p)(\hat{m}_q-m_q)}{\sigma^{p+q}\sqrt{g_{p,p}(\rho,N)g_{q,q}(\rho,N)}}\right)\right)}{2\pi\sigma^{p+q}\sqrt{g_{p,p}(\rho,N)g_{q,q}(\rho,N)(1-\xi^2(\rho,N))}}.\end{aligned} \tag{29}$$

$$\begin{aligned}&\frac{p\left(\hat{m}_p^2\sigma^{-2p}-\hat{m}_pf_p(\rho)\sigma^{-p}\right)}{g_{p,p}(\rho,N)}+\frac{q\left(\hat{m}_q^2\sigma^{-2q}-\hat{m}_qf_q(\rho)\sigma^{-q}\right)}{g_{q,q}(\rho,N)}\\ &-\frac{\xi(\rho,N)\left((p+q)\hat{m}_p\hat{m}_q\sigma^{-(p+q)}-q\hat{m}_qf_p(\rho)\sigma^{-q}-p\hat{m}_pf_q(\rho)\sigma^{-p}\right)}{\sqrt{g_{p,p}(\rho,N)g_{q,q}(\rho,N)}}=-\sqrt{1-\xi^2(\rho,N)}(p+q).\end{aligned} \tag{30}$$

where $F(\rho)=\frac{f_p^q(\rho)}{f_q^p(\rho)}$. Therefore, $\hat{F}$ is approximately a Gaussian random variable with pdf

$$\psi(\hat{F}|\rho)=\frac{1}{\sqrt{2\pi\nu_F(\rho,N)}}\exp\left(-\frac{\left(\hat{F}-F(\rho)\right)^2}{2\nu_F(\rho,N)}\right). \tag{33}$$

The approximate ML estimator for ρ can be obtained by maximizing $\psi(\hat{F}|\rho)$ over ρ. A remarkable property of $\psi(\hat{F}|\rho)$ is that it depends on ρ only but not on σ. Therefore, the estimations of ρ and σ are decoupled.

After obtaining ρ^* from maximizing $\psi(\hat{F}|\rho)$, we can substitute it into (30) and estimate σ. We can use only either $\hat{m}_p$ or $\hat{m}_q$ to estimate σ, so that the complexity is reduced. For example, we consider $\hat{m}_p$ as Gaussian with pdf

$$\psi(\hat{m}_p|\rho,\sigma)=\frac{1}{\sqrt{2\pi\nu_p}}\exp\left(-\frac{(\hat{m}_p-m_p)^2}{2\nu_p}\right), \tag{34}$$

where ν_p is defined in (28). Maximizing $\psi(\hat{m}_p|\rho,\sigma)$ over σ gives the ML estimate of σ as

$$\sigma^*=\sqrt[p]{\frac{2\hat{m}_p}{f_p(\rho^*)+\sqrt{f_p^2(\rho^*)+4g_{p,p}(\rho^*,N)}}}. \tag{35}$$

Comparing (35) with the direct estimator (26), we find that the former reduces to the latter if we choose $g_{p,p}(\rho^*,N)=0$ in (35), i.e., if $N\to\infty$. Therefore, the direct estimator is asymptotically ML. From (30), we can see that the true ML estimate σ depends on both $\hat{m}_p$ and $\hat{m}_q$. Let σ_p^* and σ_q^* denote the solution of (35) using $\hat{m}_p$ and $\hat{m}_q$, respectively. We can use a linear combination of σ_p^* and σ_q^*, i.e., $(1-\gamma)\sigma_p^*+\gamma\sigma_q^*$ as the final estimate.

4) Pseudo LMMSE Estimator: We next consider another popular estimator: the linear MMSE. From the direct estimator, we obtain

$$\begin{aligned}\hat{\rho}=&F^{-1}\left(\frac{(m_p+\epsilon_p)^q}{(m_q+\epsilon_q)^p}\right)\approx\rho+\frac{1}{F'(\rho)}\left(\frac{qm_p^{q-1}}{m_q^p}\epsilon_p-\frac{pm_p^q}{m_q^{p+1}}\epsilon_q\right)\\ =&\rho+\frac{1}{q\frac{f_p'(\rho)}{f_p(\rho)}-p\frac{f_q'(\rho)}{f_q(\rho)}}\left(\frac{q}{\sigma^pf_p(\rho)}\epsilon_p-\frac{p}{\sigma^qf_q(\rho)}\epsilon_q\right),\\ \hat{\sigma}=&\sqrt[p]{\frac{m_p+\epsilon_p}{f_p(\rho+\epsilon_\rho)}}\approx\sigma+\frac{1}{p}\left(\frac{1}{\sigma^{p-1}f_p(\rho)}\epsilon_p-\frac{\sigma f_p'(\rho)}{f_p(\rho)}\epsilon_\rho\right),\end{aligned} \tag{36}$$

where ϵ_ρ is the error between $\hat{\rho}$ and ρ. The variances of ρ and σ can be computed as

$$\begin{aligned}\nu_\rho(\rho,N)=&E\left\{\frac{\left(\frac{q}{\sigma^pf_p(\rho)}\epsilon_p-\frac{p}{\sigma^qf_q(\rho)}\epsilon_q\right)^2}{\left(q\frac{f_p'(\rho)}{f_p(\rho)}-p\frac{f_q'(\rho)}{f_q(\rho)}\right)^2}\right\}\\ =&\frac{\frac{q^2g_{p,p}(\rho,N)}{f_p^2(\rho)}+\frac{p^2g_{q,q}(\rho,N)}{f_q^2(\rho)}-\frac{2pqg_{p,q}(\rho,N)}{f_p(\rho)f_q(\rho)}}{\left(q\frac{f_p'(\rho)}{f_p(\rho)}-p\frac{f_q'(\rho)}{f_q(\rho)}\right)^2},\end{aligned} \tag{37}$$

and

$$\begin{aligned}\nu_\sigma(\rho,N)=&E\left\{\frac{\left(\frac{f_q'(\rho)}{\sigma^p}\epsilon_p-\frac{f_p'(\rho)}{\sigma^q}\epsilon_q\right)^2}{\left(qf_q(\rho)f_p'(\rho)-pf_p(\rho)f_q'(\rho)\right)^2}\right\}\\ =&\frac{f_q'^2(\rho)g_{p,p}(\rho,N)+f_p'^2(\rho)g_{q,q}(\rho,N)-2f_p'(\rho)f_q'(\rho)g_{p,q}(\rho,N)}{\left(qf_q(\rho)f_p'(\rho)-pf_p(\rho)f_q'(\rho)\right)^2}.\end{aligned} \tag{38}$$

The MMSE estimator then takes the form

$$\hat{\rho}=\alpha F^{-1}\left(\frac{(\hat{m}_p)^q}{(\hat{m}_q)^p}\right),\quad \hat{\sigma}=\beta\sqrt[p]{\frac{\hat{m}_p}{f_p(\hat{\rho})}}, \tag{39}$$

where α and β are two scalers to be determined. To find α, we minimize the MSE between ρ and $\hat{\rho}$, i.e., $E\{|\rho-\hat{\rho}|^2\}$, which gives

$$\alpha(\rho,N)=\frac{\rho^2}{\rho^2+\nu_\rho(\rho,N)}, \tag{40}$$

where $\nu_\rho(\rho,N)$ is defined in (37). By substituting (40) into (39), ρ can be found from the root of

$$\hat{\rho}=\alpha(\hat{\rho},N)F^{-1}\left(\frac{(\hat{m}_p)^q}{(\hat{m}_q)^p}\right). \tag{41}$$

From the expression of $\hat{\sigma}$ in (36) and the definition $\epsilon_\rho=\hat{\rho}-\rho$, if $\alpha=1$, we can write $\hat{\sigma}$ in (39) as

$$\hat{\sigma}\approx\beta\sigma+\beta\frac{\sigma}{qf_q(\rho)f_p'(\rho)-pf_q(\rho)f_q'(\rho)}\left(\frac{f_q'(\rho)}{\sigma^p}\epsilon_p+\frac{f_p'(\rho)}{\sigma^q}\epsilon_q\right). \tag{42}$$

By minimizing the MSE $E\{(\hat{\sigma}-\sigma)^2\}$, we obtain

$$\beta(\rho,N)=\frac{1}{1+\nu_\sigma(\rho,N)}. \tag{43}$$

Finally, substituting (43) into (39), we get

$$\hat{\sigma} = \beta(\rho, N) \sqrt[p]{\frac{\hat{m}_p}{f_p(\hat{\rho})}} \approx \beta(\hat{\rho}, N) \sqrt[p]{\frac{\hat{m}_p}{f_p(\hat{\rho})}}, \tag{44}$$

where $\hat{\rho}$ is from (41). Interestingly, the LMMSE estimator can be seen as an approximation of the ML estimator (38) when $\nu_\sigma(\rho, N)$ is small. As the true LMMSE estimator requires substituting the true ρ into (40) and (43), the derived MMSE estimators are named as pseudo LMMSE estimators.

Remarks:

- The SNV estimator in [9] or (14) is a special case of (25) if we choose $P = 2$, $k_1 = k_2 = 1$, and $Q = 1$, $\kappa_1 = 2$. The second- and the fourth-order moments M_2M_4 estimator in [9] is obtained by choosing $P = 2$, $k_1 = k_2 = 2$, and $Q = 1$, $\kappa_1 = 4$ in (25). However, unlike the SNV in [9] which utilizes (14) to estimate the SNR directly, our method uses inverse function F^{-1} to compute the SNR. Moreover, unlike the M_2M_4 estimator in [9] which estimates h, σ first and then computes ρ, our method estimates ρ directly from (25).
- Even though the proposed estimators seem to involve complicated function evaluation, they can be implemented in practice by building a look-up table.

C. Modulation Mismatch and Uniform Approximation

The proposed estimators require knowledge of the modulation format used by the primary user. If the secondary user is used at a specific primary application with known modulation, the proposed estimators can be directly used. However, if the secondary user is operated at an arbitrary primary application, the proposed estimators may incur a modulation mismatch problem. One possible solution is to apply the proposed estimators with the largest possible size of the modulation constellation used by the primary user. In the extreme case, we consider that the constellation $\mathcal{C}$ contains an infinite number of signal points, where each point is uniformly distributed over $[-\sqrt{3}, \sqrt{3}]$ and $\sqrt{3}$ is chosen to keep the average power unit. Then $E\{|y_i|^k\}$ can be computed by replacing the summation over x_i in (19) with an integral over $[-\sqrt{3}, \sqrt{3}]$, i.e., (45) at the top of the next page.

Specifically, when k is even, we can simplify (45) as

$$E\{|y_i|^k\} = \frac{1}{6} \int_{-\sqrt{\frac{3}{2}}}^{\sqrt{\frac{3}{2}}} \int_{-\sqrt{\frac{3}{2}}}^{\sqrt{\frac{3}{2}}} \sum_{j=0}^{\frac{k}{2}} \binom{\frac{k}{2}}{j} G(hu, 2j, \sigma) G(hv, k-2j, \sigma) du dv, \tag{46}$$

where $G(hz, 2j, \sigma)$ is defined in (21), and

$$E\{|y_i|^k\} = \sum_{j=0}^{\frac{k}{2}} \binom{\frac{k}{2}}{j} F(h, 2j, \sigma) F(h, k-2j, \sigma), \tag{47}$$

where

$$\begin{aligned} F(h, k, \sigma) &= \frac{1}{\sqrt{6}} \int_{-\sqrt{\frac{3}{2}}}^{\sqrt{\frac{3}{2}}} G(hz, k, \sigma) dz \\ &= \sum_{j=0}^{k/2} \frac{1}{k-2j+1} \binom{k}{2j} \left(\frac{3h^2}{2}\right)^{\frac{k}{2}-j} \frac{(2j)!}{2^{2j} j!} \sigma^{2j}. \end{aligned} \tag{48}$$

The estimators in Section III-A and Section III-B can be used with (45) and (47).

When k is odd, however, closed-form $E\{|y_i|^k\}$ is not available, we need to evaluate (45) numerically.

We can even obtain closed form ML estimator under the uniform assumption, e.g., (8) can be rewritten as

$$\begin{aligned} p(y_1, \ldots, y_N | h, \sigma) &= \frac{1}{(12\pi)^N \sigma^{2N}} \\ &\times \prod_{i=1}^{N} \int_{-\sqrt{\frac{3}{2}}}^{\sqrt{\frac{3}{2}}} \int_{-\sqrt{\frac{3}{2}}}^{\sqrt{\frac{3}{2}}} \exp\left(-\frac{|y_i - h(u_i + jv_i)|^2}{\sigma^2}\right) du_i dv_i. \end{aligned} \tag{49}$$

The approximate ML estimates can be obtained by maximizing (48) over h and σ, which possibly could be solved by performing a local search near the point obtained by the estimators in Section III-A and Section III-B. However, this estimator depends on $y_1, \ldots, y_N$ in a complicated way, and is hard to implement in practice.

Intuitively, the performance of the estimators that use the uniform approximation is a worst-case bound. The proposed estimators can also be extended to the higher-order PSK (phase shift keying) case, where we can approximate the PSK constellation by using a uniform distribution on the unit circle, i.e., $e^{j\theta}$ and θ is uniformly distributed over $[0, 2\pi)$.

D. Blind Spectrum Sensing

There are two methods of blind energy detection. In the first method, the estimated h and σ are used without taking into account the history of the noise variance estimation. In the second method, the noise variance is estimated by using the previous estimates, assuming that the noise variances is constant over time. The energy detector is then applied as in Section II.

For the first method, the estimated SNR $\hat{\rho}$ is compared with a threshold λ. If $\hat{\rho} > \lambda$, the secondary user decides that $\hat{\theta} = 1$; otherwise, $\hat{\theta} = 0$. The estimate $\hat{\rho}$ can be obtained from the direct estimator (25). We need the distribution of $\hat{\rho}$ to compute the false alarm probability. For this, we can approximate $\hat{\rho}$ by using (36) as a Gaussian random variable. The false alarm probability can then be approximated as

$$P_f = \Pr(\hat{\theta} = 1 | \theta = 0) = Q\left(\frac{\lambda}{\sqrt{\nu_\rho(0, N)}}\right), \tag{50}$$

where $\nu_\rho(0, N)$ is defined in (37). Similarly, the detection probability is

$$P_d = \Pr(\hat{\theta} = 1 | \theta = 1) = Q\left(\frac{\lambda - \rho}{\sqrt{\nu_\rho(\rho, N)}}\right). \tag{51}$$

The second method consists of two parts: estimating the noise variance and tracking the noise variance estimate. Let $\hat{\sigma}_n^2$ denote the n-th noise variance estimate. To smooth the estimation of the noise variance, we can use the time average as

$$\bar{\sigma}^2 = \frac{1}{K} \sum_{n=1}^{K} \hat{\sigma}_n^2. \tag{52}$$

$$E\{|y_i|^k\} = \frac{h^k}{6\cdot 2^{\frac{k}{2}}}\rho^{-\frac{k}{2}}\Gamma\left(\frac{k}{2}+1\right)\int_{-\sqrt{\frac{3}{2}}}^{\sqrt{\frac{3}{2}}}\int_{-\sqrt{\frac{3}{2}}}^{\sqrt{\frac{3}{2}}}\exp\left(-\rho(u^2+v^2)\right){}_1F_1\left(\frac{k}{2}+1;1;\rho(u^2+v^2)\right)dudv. \tag{45}$$

Alternatively, we can smooth the noise variance estimate by using a first-order infinite impulse response (IIR) filter

$$\bar{\sigma}^2 = (1-\gamma)\bar{\sigma}^2 + \gamma\hat{\sigma}_n^2, \tag{53}$$

where $1 > \gamma > 0$ is a smoothing parameter.

Aided by the energy detector in Section II, we compare $\sum_{i=1}^{N}|y_i|^2$ with a threshold $\lambda\bar{\sigma}^2$. If $|y|^2 > \lambda$, the secondary user decides $\hat{\theta} = 1$; otherwise, $\hat{\theta} = 0$. The parameter λ is chosen such that the false alarm probability is ζ, i.e., $P_f(\lambda) = \zeta$.

Then, we can either use (5) directly or take into account the estimation error in $\bar{\sigma}^2$. Assuming that the variance of the estimate $\hat{\sigma}_n^2$ is $\sigma^4\nu_{\sigma,n}$ and the variance of $\bar{\sigma}^2$ is $\sigma^4\nu_{\bar{\sigma}}$, from (53) we obtain

$$\nu_{\bar{\sigma}} = (1-\gamma)^2\nu_{\bar{\sigma}} + \gamma^2\nu_{\sigma,n}, \tag{54}$$

where $\nu_{\sigma,n}$ can be found from Section III-B. Let $\bar{\sigma}^2 = \sigma^2+\epsilon_\sigma$, where ϵ_σ is a Gaussian random variable with zero mean and variance $\sigma^4\nu_{\bar{\sigma}}$. We then substitute $\bar{\sigma}^2$ into (5) and obtain

$$\begin{aligned}P_f(\lambda) =& \frac{1}{\sqrt{2\pi\sigma^2\nu_{\bar{\sigma}}}}\int_{-\infty}^{\infty}\int_{\lambda(\sigma^2+\epsilon_\sigma)}^{+\infty}\frac{t^{N-1}}{\sigma^{2N}\Gamma(N)}e^{-\frac{t}{\sigma^2}-\frac{\epsilon_\sigma^2}{2\sigma^4\nu_{\bar{\sigma}}}}dt\\ =& \frac{1}{\sqrt{2\pi\nu_{\bar{\sigma}}}\Gamma(N)}\int_{-\infty}^{\infty}\Gamma\left(N,\lambda(1+x)\right)e^{-\frac{x^2}{2\nu_{\bar{\sigma}}}}dx.\end{aligned} \tag{55}$$

IV. Performance Analysis and Optimization

A. Cramér-Rao Bound

In the literature, the results for the CRB are derived for ρ only, see, e.g., [9]. In this paper, we are interested in the CRB for both h and σ. This CRB can be obtained by computing

$$\begin{aligned}d_1 =& \frac{\partial\log p\left(y_1,\ldots,y_N|h,\sigma\right)}{\partial h}\\ =& \sum_{i=1}^{N}\frac{\sum_{x_i\in\mathcal{C}}\Pr(x_i)\frac{(y_i-hx_i)x_i}{\sigma^2}\exp\left(-\frac{(y_i-hx_i)^2}{2\sigma^2}\right)}{\sum_{x_i\in\mathcal{C}}\Pr(x_i)\exp\left(-\frac{(y_i-hx_i)^2}{2\sigma^2}\right)},\end{aligned} \tag{56}$$

and

$$\begin{aligned}d_2 =& \frac{\partial\log p\left(y_1,\ldots,y_N|h,\sigma\right)}{\partial\sigma}\\ =& \sum_{i=1}^{N}\frac{\sum_{x_i\in\mathcal{C}}\Pr(x_i)\frac{(y_i-hx_i)^2}{\sigma^3}\exp\left(-\frac{(y_i-hx_i)^2}{2\sigma^2}\right)}{\sum_{x_i\in\mathcal{C}}\Pr(x_i)\exp\left(-\frac{(y_i-hx_i)^2}{2\sigma^2}\right)} - \frac{N}{\sigma},\end{aligned} \tag{57}$$

where $p\left(y_1,\ldots,y_N|h,\sigma\right)$ is defined in (8). The true CRB is thus [13]

$$\begin{aligned}\mathrm{var}(h) \geq \mathrm{CRB}_h &= \frac{E_{y_i}\{d_2^2\}}{E_{y_i}\{d_1^2\}E_{y_i}\{d_2^2\} - E_{y_i}^2\{d_1d_2\}},\\ \mathrm{var}(\sigma) \geq \mathrm{CRB}_\sigma &= \frac{E_{y_i}\{d_1^2\}}{E_{y_i}\{d_1^2\}E_{y_i}\{d_2^2\} - E_{y_i}^2\{d_1d_2\}}.\end{aligned} \tag{58}$$

Since deriving the true CRB in closed-form appears intractable, we resort to the modified CRB (MCRB) in [14], which can be computed as

$$d_1(\mathbf{x}) = \frac{\partial\log p\left(\mathbf{y}|\mathbf{x},h,\sigma\right)}{\partial h} = \sum_{i=1}^{N}\frac{(y_i-hx_i)x_i}{\sigma^2}, \tag{59}$$

and

$$d_2(\mathbf{x}) = \frac{\partial\log p\left(\mathbf{y}|\mathbf{x},h,\sigma\right)}{\partial\sigma} = \sum_{i=1}^{N}\frac{(y_i-hx_i)^2}{\sigma^3} - \frac{N}{\sigma}, \tag{60}$$

where $\mathbf{y} = [y_1,\ldots,y_N]^T$ and $\mathbf{x} = [x_1,\ldots,x_N]^T$. The modified CRB is thus [14]

$$\begin{aligned}&\mathrm{var}(h) \geq \mathrm{MCRB}_h\\ =&\frac{E_{x_i,y_i}\{d_2^2(\mathbf{x})\}}{E_{x_i,y_i}\{d_1^2(\mathbf{x})\}E_{x_i,y_i}\{d_2^2(\mathbf{x})\} - E_{x_i,y_i}^2\{d_1(\mathbf{x})d_2(\mathbf{x})\}} = \frac{\sigma^2}{N},\\ &\mathrm{var}(\sigma) \geq \mathrm{MCRB}_\sigma\\ =&\frac{E_{x_i,y_i}\{d_1^2(\mathbf{x})\}}{E_{x_i,y_i}\{d_1^2(\mathbf{x})\}E_{x_i,y_i}\{d_2^2(\mathbf{x})\} - E_{x_i,y_i}^2\{d_1(\mathbf{x})d_2(\mathbf{x})\}} = \frac{\sigma^2}{2N}.\end{aligned} \tag{61}$$

From [14], the modified CRB is also a lower bound of the CRB. Hence, the relationship

$$\begin{aligned}\mathrm{var}(h) \geq \mathrm{CRB}_h \geq \mathrm{MCRB}_h = \frac{\sigma^2}{N},\\ \mathrm{var}(\sigma) \geq \mathrm{CRB}_\sigma \geq \mathrm{MCRB}_\sigma = \frac{\sigma^2}{2N}.\end{aligned} \tag{62}$$

The modified CRB for SNR or ρ is given by [9, (64)] as

$$\mathrm{MCRB}_\rho = \frac{2\rho}{N} + \frac{\rho^2}{N}. \tag{63}$$

B. Optimization of Moment Pair

The moment based estimators in Section III-B are close to the optimum only for BPSK. For a general constellation, we may choose a different moment pair $\hat{m}_p$ and $\hat{m}_q$ to optimize the performance. We consider minimizing the estimation variance given in Section III-B. Our experiments indicate that the performance of estimating σ depends heavily on the accuracy of $\hat{\rho}$. This finding suggests minimizing the variance of $\hat{\rho}$ in (37). The optimal moment pair can be found by minimizing (37) over different moment values.

Fig. 1 compares the variance of ρ with different moment pairs for 64QAM with $N = 1344$. The figure shows that the optimal moment pair depends on SNR ρ. Unlike BPSK where $p = 1$ and $q = 2$ converge to the optimal solution, the moment-based estimators diverge from the optimal solution for each fixed moment pair in high SNR. In low SNR, a small pair $p = 2$ and $q = 4$ achieves the minimum variance, while a large pair $p = k$ and $q = k+1$ generally achieves the minimum variance in high SNR, where k increases as ρ increases. Interestingly, the envelope of the moment pairs is flat in high SNR, indicating that the average MSE of ρ has the form $B(N,\mathcal{C})/\rho^2$ where $B(N,\mathcal{C})$ is a constant depending

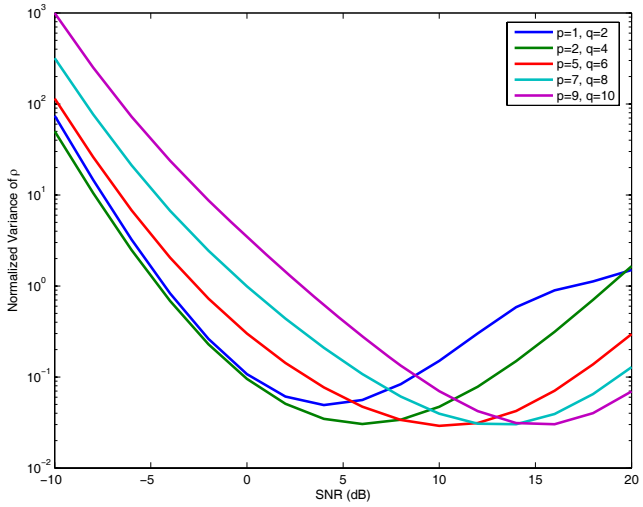

Fig. 1. Comparison of variance of ρ for different moment pairs for 64QAM with $N = 1344$.

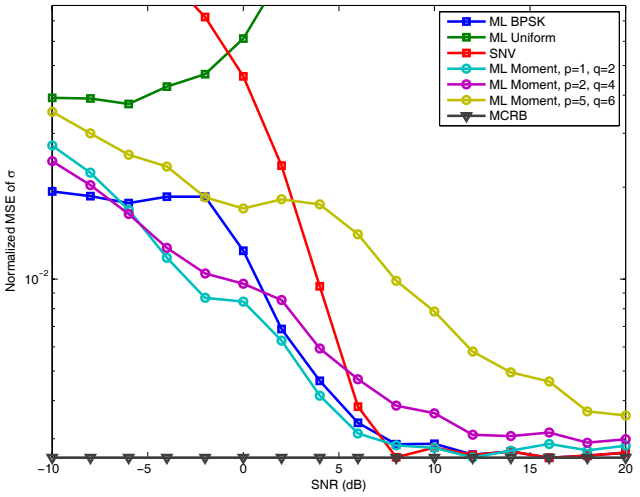

Fig. 3. Comparison of normalized MSE for σ between different estimators with BPSK and $N = 192$.

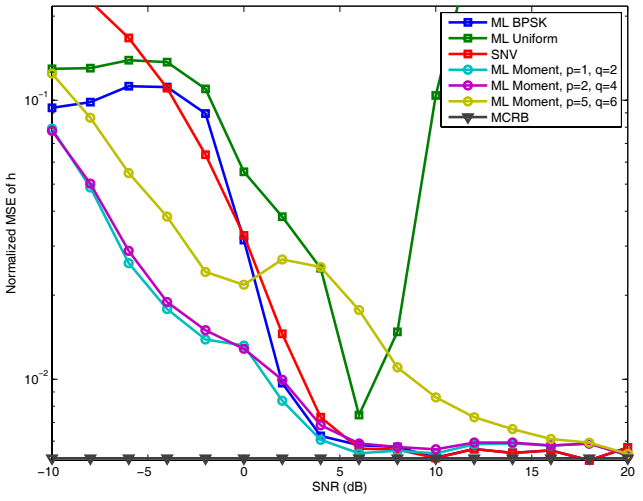

Fig. 2. Comparison of normalized MSE for h between different estimators with BPSK and $N = 192$.

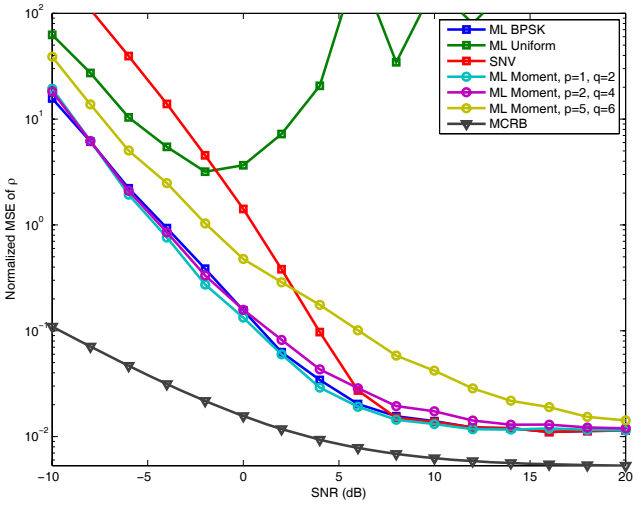

Fig. 4. Comparison of normalized MSE for ρ between different estimators with BPSK and $N = 192$.

on the number of samples and the modulation constellation. Comparing with the modified CRB in (62) and noting that the modified CRB is a lower bound on the performance of the ML estimator, we observe that the performance of the ML estimator can be achieved within a constant factor by using a high moment pair as ρ increases. One possible way to implement this is to use a low-order moment pair to get a crude estimate of ρ and then choose another moment pair to minimize the variance according to this estimate.

V. Simulation Results

In this section, we present our simulation results to complement our theoretical analysis. We estimate h and σ by using $N = 192$ and $N = 1344$ samples. These numbers are chosen in compliance with WCDMA standard [12], where h and σ are estimated every 192 symbols or 0.4 ms. The constellations of BPSK, 16QAM and 64QAM are simulated. The ML estimator for BPSK by using (9) is denoted as the "ML BPSK"; the estimator using (14) is denoted as the SNV; the uniform approximation by maximizing (48) is denoted as the "ML Uniform"; the moment ML estimator by maximizing (29) is denoted as the "ML Moment"; the estimator by using (26) is denoted as "Direct Moment"; the estimator using (33) and (35) is denoted as the "Approximate ML Moment". The simulation is carried out for SNR between -10 dB and 20 dB. We restrict the maximum ρ to be 10^3 in the moment estimators.

We first show the simulation results for the estimation of h, σ and ρ. The normalized MSE (NMSE) is adopted as the performance metric, which is defined as $E\{|\hat{h}-h|^2\}/h^2$ for h, $E\{|\hat{\sigma}-\sigma|^2\}/\sigma^2$ for σ, and $E\{|\hat{\rho}-\rho|^2\}/\rho^2$ for ρ. The NMSEs are obtained after 2000 simulation runs for each SNR.

Fig. 2–F.g 4 show the NMSEs of h, σ and ρ with BPSK and $N = 192$, respectively. We find that except the ML Uniform estimator, all the other estimators can achieve the CRBs of h, σ and ρ in high SNR. As the uniform approximation is weak for BPSK, the performance of the ML Uniform is not good. Figs. 2–Fig. 4 reveal that the moment estimators with $p = 1$ and $q = 2$ perform better than higher moments. The reason is that the $p = 1$ and $q = 2$ estimator is approximately ML as

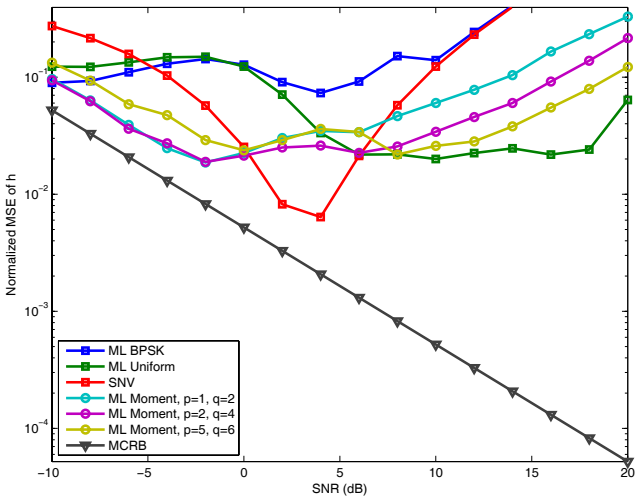

Fig. 5. Comparison of normalized MSE for h between different estimators with 64QAM and $N = 192$.

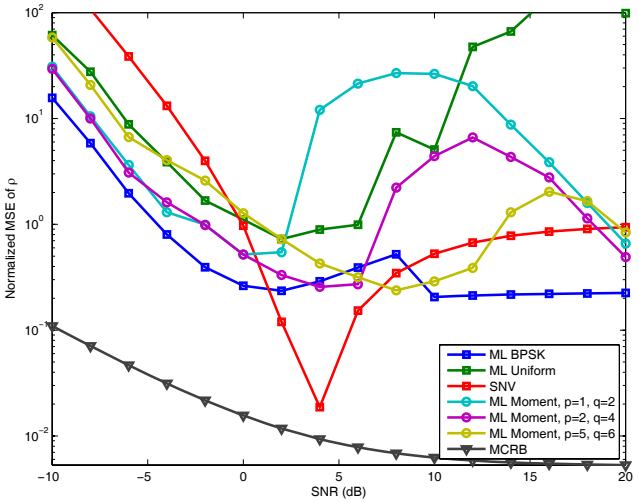

Fig. 7. Comparison of normalized MSE for ρ between different estimators with 64QAM and $N = 192$.

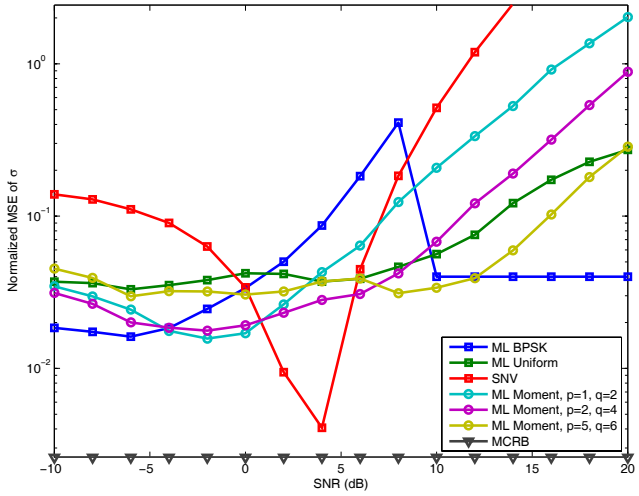

Fig. 6. Comparison of normalized MSE for σ between different estimators with 64QAM and $N = 192$.

shown in Section III-A. Although the SNV estimator performs similar to the ML BPSK in high SNR, it performs worse than the later in low SNR.

Fig. 5- Fig. 7 demonstrate the NMSEs of h, σ and ρ with 64QAM and $N = 192$, respectively. For both h and σ, all the estimators' NMSEs diverge, but the MSEs converge to zero as SNR goes to infinity because it is clear that the proposed estimators' estimates converge to their true values as SNR goes to infinity, which can also be seen from Fig. 1. For ρ, the moment based estimators converge because in the estimator of ρ we add an additional constraint that the estimated ρ must be smaller than 30 dB. Interestingly, the NMSEs of ρ and σ obtained by using ML BPSK are still good though the NMSE of h is not good. This can be explained as follows. The BPSK approximation of the amplitude of 64QAM is not accurate. As in Fig. 1, we find that the high moment estimator with $p = 5$ and $q = 6$ achieve better performance than those with smaller moments in high SNR. These findings confirm that to achieve better performance in high SNR, a high moment pair is required. The peaks of the ML moment estimator are due to the use of the NMSE metric and the upperbound 30 dB on ρ. When comparing Fig. 1 with Fig. 5- Fig. 7, we can see that as the moment pair order increases, the proposed algorithms perform better with increasing moment order. If there is no constraint on ρ, we expect to see that the normalized variances of the moment based estimators will diverge for high order QAM. In practice, choosing the upper bound on ρ (here 30 dB) depends on the application environment.

When comparing the performance of ML Uniform in Fig. 3 with Fig. 6, we observe that ML Uniform achieves better performance for 64QAM than BPSK. The reason is that 64QAM has more constellation points in each dimension than BPSK, which is implied by the fact that the former is more similar to the uniform distribution than to the latter.

Fig. 8 shows the NMSE of σ for ML Moment with different constellations. As SNR increases, the performance of higher order constellation degrades faster for both moment pairs. By increasing the moment order, the performance of both 16QAM and 64QAM becomes better. In high SNR, the higher order constellation achieves a worse performance.

Next, we apply the noise variance estimator to spectrum sensing. To evaluate the effect of estimation error on the performance of spectrum sensing, we model the estimated noise variance $\hat{\sigma}^2$ as a Gaussian random variable with mean σ^2 and variance $\sigma^4 \nu_{\bar{\sigma}}$, where $\nu_{\bar{\sigma}}$ is equal to the normalized MSE. The energy detector is used along with the estimated noise variance. We compare the traditional spectrum sensing that computes the detection threshold λ by substituting $\hat{\sigma}^2$ into (5) with the proposed algorithm that compute λ by using (55). In addition, we include the result from the ML BPSK estimator, where the estimated noise variance and the signal power are averaged from 1000 runs. Simulations are performed at SNR$= -5$ dB with 16QAM and $N = 48$. Fig. 9 shows the achieved false alarm probability P_f given a target P_f. As the proposed algorithms achieve almost the same P_f, we only show P_f with the ML BPSK estimator. We find that the traditional method of using the estimated noise variance directly increases the false alarm probability

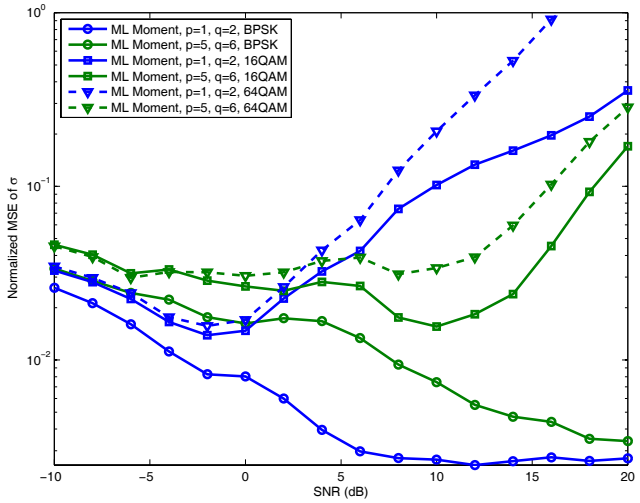

Fig. 8. Comparison of normalized MSE for σ using the moment estimator for different constellations ($N = 192$).

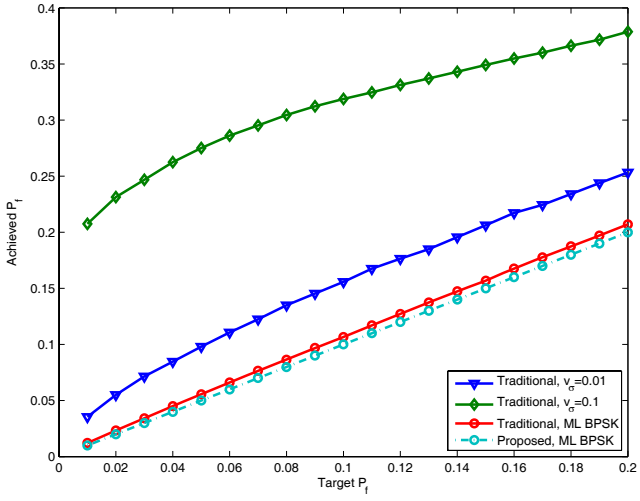

Fig. 9. Comparison of achieved false alarm probability P_f with 16QAM and $N = 48$ at SNR$= -5$ dB.

P_f especially when $\nu_{\bar{\sigma}}$ is large, while the proposed algorithm can achieve the desired P_f. This result shows that computing P_f in the conventional energy detector depends crucially on the accuracy of the noise variance estimate. In Fig. 10, we compare the achievable correct detection probability P_d of different algorithms given a target P_f. We can see that the good behavior of P_f using (55) is at the expense of a smaller P_d. The traditional algorithm using (5) achieves a greater P_d when $\nu_{\bar{\sigma}}$ is small but it cannot meet the regulation of P_f. As the proposed noise variance and signal power estimators can achieve a very high accuracy, the impact of the estimation error on the performance of the proposed spectrum sensing algorithm is negligible from Figs. 9 and Fig. 10.

VI. Conclusion

In this paper, we considered blind energy detection based spectrum sensing without knowing *a priori* the signal power of the primary user and the noise variance. We proposed three estimators, i.e., the direct estimator, the approximate ML

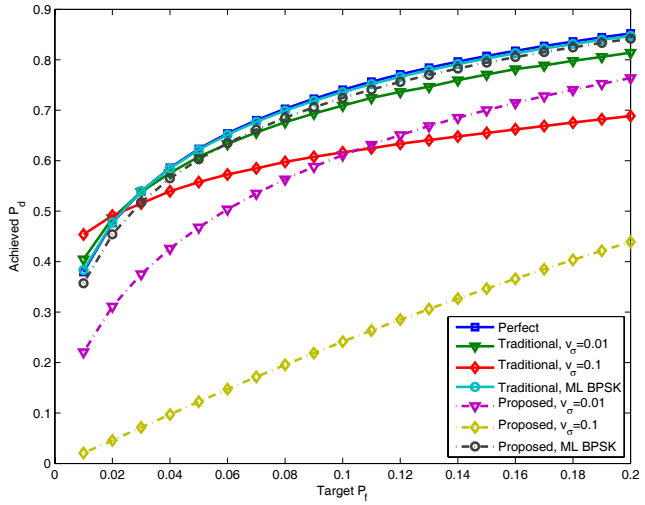

Fig. 10. Comparison of achieved correct detection probability P_d with 16QAM and $N = 192$ at SNR$= -5$ dB.

estimator, and the pseudo linear MMSE estimator by using the moments of the received signals at the secondary user. The proposed estimators exploit the finite signal constellation of the primary user. When this constellation is unknown to the secondary user, we proposed to use a continuous uniform distribution to approximate and developed a robust estimator. The CRB was also derived. We also discussed the way to find the optimal moment pair and to choose the spectrum sensing detection threshold under the estimation error. The proposed estimators may also be profitably employed in conventional applications such as SNR estimation and turbo decoding.

References

[1] J. Mitola and G. Maguire, "Cognitive radio: making software radios more personal," *IEEE Personal Commun.*, vol. 6, no. 4, pp. 13-18, Aug. 1999.

[2] D. Cabric, A. Tkachenko, and R. W. Brodersen, "Spectrum sensing measurements of pilot, energy, and collaborative detection," in *Proc. IEEE MILCOM*, Oct. 2006, pp. 1-7.

[3] Y.-C. Liang, Y. Zeng, E. C. Y. Peh, and A. T. Hoang, "Sensing-throughput tradeoff for cognitive radio networks," *IEEE Trans. Wireless Commun.*, vol. 7, no. 4, pp. 1326-1337, Apr. 2008.

[4] D.-C. Oh and Y.-H. Lee, "Energy detection based spectrum sensing for sensing error minimization in cognitive radio networks," *International J. Commun. Netw. Inf. Security*, vol. 1, no. 1, pp. 1-5, Apr. 2009.

[5] C. da Silva, B. Choi, and K. Kim, "Distributed spectrum sensing for cognitive radio systems," in *Proc. Inf. Theory Applications Workshop*, 2007.

[6] M. Gandetto and C. Regazzoni, "Spectrum sensing: a distributed approach for cognitive terminals," *IEEE J. Sel. Areas Commun.*, vol. 25, no. 3, pp. 546-557, Apr. 2007.

[7] W. Gardner and C. Spooner, "Signal interception: performance advantages of cyclic-featuredetectors," *IEEE Trans. Commun.*, vol. 40, no. 1, pp. 149-159, Jan. 1992.

[8] Z. Tian and G. B. Giannakis, "A wavelet approach to wideband spectrum sensing for cognitive radios," in *Proc. Int. Conf. Cognitive Radio Oriented Wireless Netw. Commun.*, June 2006, pp. 1-5.

[9] D. Pauluzzi and N. Beaulieu, "A comparison of SNR estimation techniques for the AWGN channel," *IEEE Trans. Commun.*, vol. 48, no. 10, pp. 1681-1691, Oct. 2000.

[10] T. Summer and S. Wilson, "SNR mismatch and online estimation in turbo decoding," *IEEE Trans. Commun.*, vol. 46, no. 4, pp. 421-423, Apr. 1998.

[11] P. Gao and C. Tepedelenlioglu, "SNR estimation for nonconstant modulus constellations," *IEEE Trans. Signal Process.*, vol. 53, no. 3, pp. 865-870, Mar. 2005.

[12] "3GPP, TR 25.214 version 7.0.0, Physical layer procedures (FDD)," Mar. 22, 2006.
[13] H. V. Poor, *An Introduction to Signal Detection and Estimation*, 2nd edition. Springer, 1998.
[14] A. N. D'Andrea, U. Mengali, and R. Reggiannini, "Modified Cramér-Rao bound and its application to synchronization problems," *IEEE Trans. Commun.*, vol. 42, no. 2-4, pp. 1391-1399, Feb.-Apr. 1994.

Tao Cui (S'04) received the M.Sc. degree in the Department of Electrical and Computer Engineering, University of Alberta, Edmonton, AB, Canada, in 2005, and the M.S. degree from the Department of Electrical Engineering, California Institute of Technology, Pasadena, USA, in 2006. He is currently working toward the Ph.D. degree at the Department of Electrical Engineering, California Institute of Technology, Pasadena. His research interests are in the interactions between networking theory, communication theory, and information theory.

Feifei Gao (S'05-M'09) received the B.Eng. degree in information engineering from Xi'an Jiaotong University, Xi'an, Shaanxi China, in 2002, the M.Sc. degree from the McMaster University, Hamilton, ON, Canada in 2004, and the Ph.D degree from National University of Singapore in 2007. He was a Research Fellow at Institute for Infocomm Research, A*STAR, Singapore in 2008. He joined the School of Engineering and Science at Jacobs University, Bremen, Germany in 2009, where he is currently an Assistant Professor. His research interests are in communication theory, broadband wireless communications, signal processing for communications, MIMO systems, and array signal processing. Mr. Gao has co-authored more than 70 refereed IEEE journal and conference papers and has served as a TPC member for IEEE ICC, IEEE GLOBECOM, IEEE VTC and IEEE PIMRC.

Jia Tang (M'06) received his B.S. and Ph.D. degree in Electrical Engineering from Xi'an Jiaotong University, Xi'an, China, and Texas A&M University, College Station, Texas, USA, in 2001 and 2006, respectively. He is currently a staff system engineer in Qualcomm Inc., Santa Clara, CA, USA, working on advanced receiver design for 3G/4G wireless communications systems. His research interests include wireless communications and networks, with emphasis on cross-layer design and optimizations, wireless QoS provisioning and wireless resource allocation.

Chintha Tellambura (SM'02) received the B.Sc. degree (with first-class honors) from the University of Moratuwa, Moratuwa, Sri Lanka, in 1986, the M.Sc. degree in electronics from the University of London, London, U.K., in 1988, and the Ph.D. degree in electrical engineering from the University of Victoria, Victoria, BC, Canada, in 1993.

He was a Postdoctoral Research Fellow with the University of Victoria (1993-1994) and the University of Bradford (1995-1996). He was with Monash University, Melbourne, Australia, from 1997 to 2002. Presently, he is a Professor with the Department of Electrical and Computer Engineering, University of Alberta. His research interests include Diversity and Fading Countermeasures, Multiple-Input Multiple-Output (MIMO) Systems and Space-Time Coding, and Orthogonal Frequency Division Multiplexing (OFDM).

Prof. Tellambura is an Associate Editor for the IEEE TRANSACTIONS ON COMMUNICATIONS and the Area Editor for Wireless Communications Systems and Theory for the IEEE TRANSACTIONS ON WIRELESS COMMUNICATIONS. He was Chair of the Communication Theory Symposium in Globecom'05 held in St. Louis, MO.